Japanese Journal of Applied Physics

The Japan Society of Applied Physics

Propagation Characteristics of Surface Acoustic Waves in $KNbO_3/SrTiO_3/Si$ Layered Structures

To cite this article: Mu-Shiang Wu Mu-Shiang Wu and Wen-Ching Shih Wen-Ching Shih 1997 *Jpn. J. Appl. Phys.* **36** 2192

Jpn. J. Appl. Phys. Vol. 36 (1997) pp. 2192–2195
Part 1, No. 4A, April 1997

Propagation Characteristics of Surface Acoustic Waves in $KNbO_3/SrTiO_3/Si$ Layered Structures

Mu-Shiang WU and Wen-Ching SHIH
Department of Electrical Engineering, Tatung Institute of Technology, Taipei 104, Taiwan, Republic of China

(Received December 2, 1996; accepted for publication January 13, 1997)

The propagation characteristics of surface acoustic waves (SAWs) in $KNObO_3/SrTiO_3/Si$ structures were investigated theoretically. Phase velocities (v_p) decrease when the hK value of the $SrTiO_3$ buffer layer increases from 0.04 to 0.2 for a specified thickness of the $KNbO_3$ film. The value of the coupling coefficient (K^2) can be as high as 10%. A layered structure with the interdigital transducer (IDT) located on top of the $KNbO_3$ film is a better choice for device fabrication if we select a coupling coefficient of 1% as a reference for comparison. The results could provide useful information for combining optical devices, semiconductor devices and SAW devices on the same Si substrate.

KEYWORDS: surface acoustic wave (SAW), $KNbO_3$ thin films, $SrTiO_3$ buffer layer, Si substrate, phase velocity, electromechanical coupling coefficient

1. Introduction

Potassium niobate ($KNbO_3$) is a promising material for optical applications such as use in frequency doublers, optical waveguides, holographic storage devices and so on.[1–8] These applications are possible due to the superior properties of $KNbO_3$, including its large electrooptic coefficient, high nonlinear optical coefficient and excellent photorefractive characteristics. Epitaxial thin films with smooth surfaces are required in order to minimize the propagation loss associated with grain boundary scattering for optical devices. It has been reported that $KNbO_3$ film with (100) orientation was successfully obtained on $SrTiO_3$ (100) single-crystal substrate by a sol-gel method[9] because lattice parameter mismatching between the $KNbO_3$ film and $SrTiO_3$ (100) single-crystal substrate is very small.

The use of $SrTiO_3$ (100) single-crystal substrate is not cost effective, and not compatible with the advancing semiconductor technology. Epitaxial growth of $KNbO_3$ film on Si is very attractive for the fabrication of optical devices and semiconductor devices on the same substrate. However, it is very difficult to prepare high-quality $KNbO_3$ film directly on Si substrate because of the lattice mismatch between them, as well as the interdiffusion of component atoms at the substrate-film interface. Therefore, the introduction of a buffer layer which is lattice-matched with both the $KNbO_3$ film and Si substrate and acts as a diffusion barrier between them is required in order to eliminate the above problems during deposition. Owing to the advances in thin-film technology, there have been many reports on the epitaxial growth of (100) $SrTiO_3$ films on Si[10–13] (001) substrates. The (100) $SrTiO_3$ buffer layer deposited on Si substrate may be used as a more inexpensive substitute for the $SrTiO_3$ (100) single-crystal substrate in order to grow epitaxial $KNbO_3$ film. This greatly increases the feasibility of fabricating integrated devices composed of optical devices and semiconductor devices.

The growth and characterization of $KNbO_3$ film for optical applications have been studied extensively. However, relatively few studies on the piezoelectric effect of $KNbO_3$ film have been carried out. The present investigation was undertaken to discuss the propagation characteristics of surface acoustic waves in $KNbO_3/SrTiO_3/Si$ structures. The layered structure we considered is $KNbO_3$(100)[001]/$SrTiO_3$(001)[100]/Si(001)[110]. The phase velocity and electromechanical coupling coefficient were calculated for the different interdigital transducer (IDT) configurations and for various thicknesses of each layer. The results could provide useful information for the further development of optical devices, semiconductor devices and SAW devices on the same Si substrate.

2. Calculations

The present theoretical analysis is an application of the theory of elastic wave propagation in thin layers, as proposed by Farnell and Adler,[14] to a $KNbO_3/SrTiO_3/Si$ three-layer structure. The coordinate system used throughout the discussion is illustrated in Fig. 1. The surface wave under consideration is assumed to propagate in the x_1 direction along a surface whose normal is in the x_3 direction and which decays exponentially in the $-x_3$ direction. The displacement and potential are considered to be independent of the x_2 direction. The equations for mechanical displacement U_i ($i = 1,2,3$) and electrical potential ϕ are

$$C_{ijkl}\frac{\partial^2 U_k}{\partial x_i \partial x_l} + e_{kij}\frac{\partial^2 \phi}{\partial x_k \partial x_i} = \rho\frac{\partial^2 U_j}{\partial t^2} \quad (1)$$

$$e_{ikl}\frac{\partial^2 U_k}{\partial x_i \partial x_l} - \varepsilon_{ik}\frac{\partial^2 \phi}{\partial x_i \partial x_k} = 0,$$
$$i,\ j,\ k,\ l = 1,\ 2,\ 3, \quad (2)$$

where C_{ijkl} is the elastic constant tensor, e_{ikl} is the piezoelectric constant tensor, ε_{ij} is the dielectric constant tensor and ρ is the mass density. The solutions to the differential equations, eq. (1) and eq. (2), are assumed to be

$$U_j = \alpha_j \exp[ikbx_3]\exp[ik(x_1 - vt)] \quad (3)$$
$$j = 1,\ 2,\ 3$$
$$\phi = \alpha_4 \exp[ikbx_3]\exp[ik(x_1 - vt)], \quad (4)$$

where k and v are the wave number and phase velocity in the x_1 direction. Usually b is taken as a com-

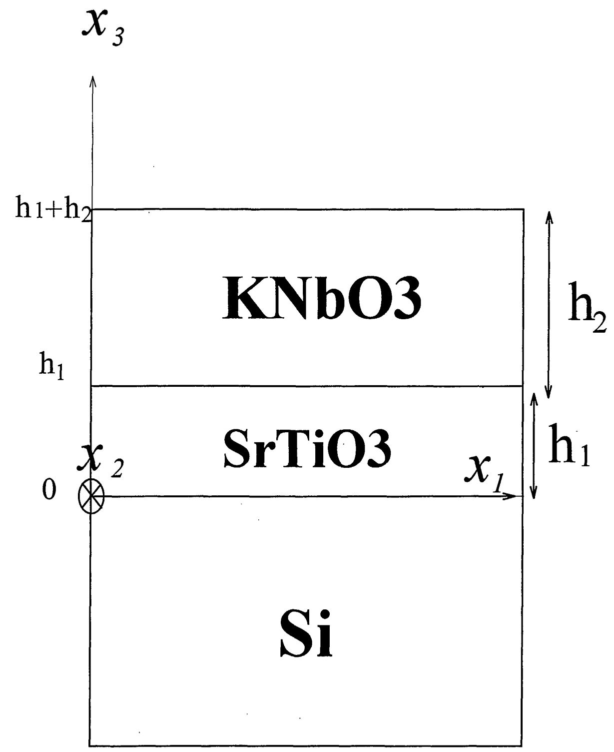

Fig. 1. Coordinate system of the three-layer structure.

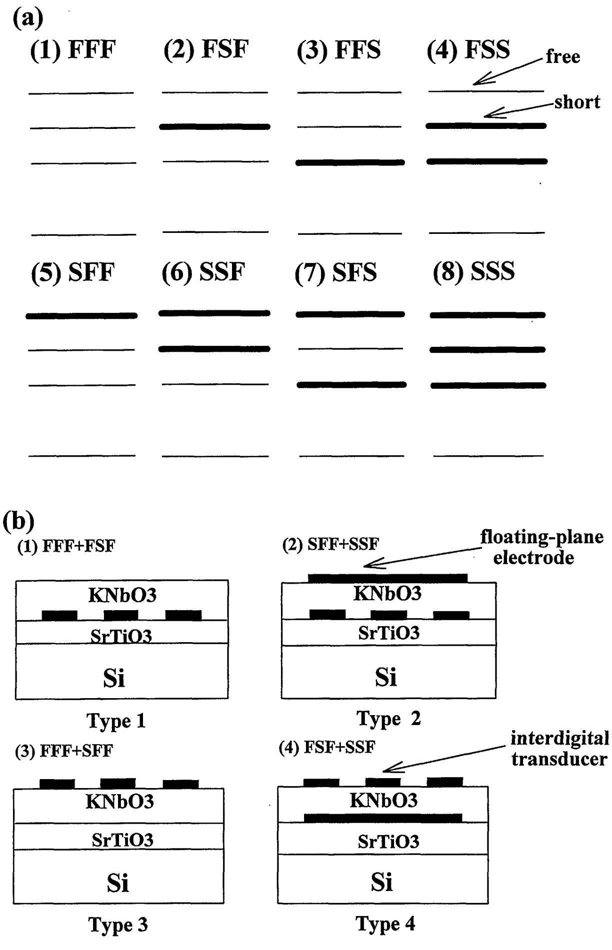

Fig. 2. (a) Prototype for electrically open and short circuits in the three-layer structure. (b) Four types of IDT configuration.

plex number, and the imaginary part of b must be negative in the substrate because the wave amplitude should evanesce in the $-x_3$ direction in the substrate. There are eight combinations of open and short circuits in the three-layer structure, as shown in Fig. 2(a). For these eight combinations, we focus our attention on four possible IDT configurations, as shown in Fig. 2(b) in order to make use of the piezoelectricity of the $KNbO_3$ film. The electromechanical coupling coefficient is obtained by using the relation $K^2 = 2(V_f - V_s)/V_f$, where V_f and V_s are the theoretical SAW velocities when the plane on which the IDT is located is electrically open and short-circuited, respectively. (001)-Cut Si wafers are selected as substrates since they are commercially available and the propagation direction in [110] is a natural cleavage plane which provides a good reference for alignment. The structure studied was $KNbO_3$(100)[001]/$SrTiO_3$(001)[100]/Si(001)[110]. For $KNbO_3$, we used the material constants listed in ref. 15 and for $SrTiO_3$ and Si, we used those listed in ref. 16. These material constants must be transformed to reflect the desired crystal cut and propagation directions.[17)]

3. Results and Discussion

In this section, the phase velocity and electromechanical coupling coefficient were calculated for different interdigital transducer (IDT) configurations and for various thicknesses of each layer. We change the hK values of the $KNbO_3$ film from 0 to 1 and fix the hK values of the $SrTiO_3$ buffer layer at 0.04, 0.08, 0.12, 0.16 and 0.2. We use the notation hK to express the normalized thickness of the film, where h is the thickness of the film, $K = 2\pi/\lambda$ is the wave number and λ is the acoustic wavelength.

3.1 *Phase velocity*

Figure 3 shows the phase velocity (v_p) dispersion curve when the hK values of the $SrTiO_3$ buffer layer are fixed at 0.04, 0.08, 0.12, 0.16 and 0.2. From Fig. 3, we can see that the phase velocities (v_p) decrease when the hK value of the KNb_3 film increases from 0 to 1 for a specified thickness of the $SrTiO_3$ buffer layer. They also decrease when the hK value of the $SrTiO_3$ buffer layer increases from 0.04 to 0.2 for a specified thickness of the $KNbO_3$

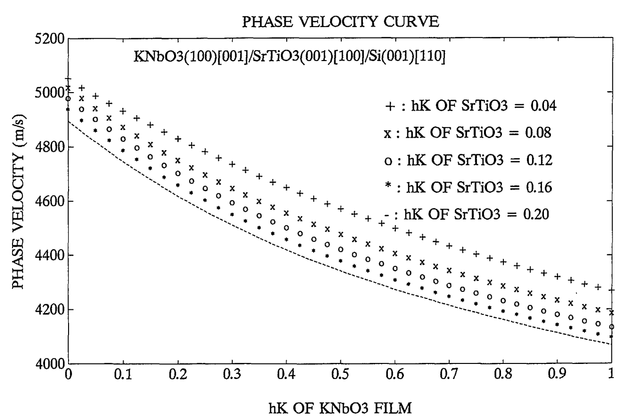

Fig. 3. Phase velocity (v_p) dispersion curve when the hK values of the $SrTiO_3$ buffer layer are fixed at 0.04, 0.08, 0.12, 0.16 and 0.2.

film.

3.2 *Coupling coefficient*

The calculated coupling coefficient (K^2) curves for different IDT configurations are shown in Figs. 4(a)–4(d) when the hK values of the $SrTiO_3$ buffer layer are fixed at 0.04, 0.08, 0.12, 0.16 and 0.2. From Fig. 4 we observe that the value of K^2 can be as high as 10% when the IDT is located at the interface between the $KNbO_3$ film and the $SrTiO_3$ buffer layer, with (type 2) and without (type 1) the floating-plane electrode on top of the $KNbO_3$ film. We also observe that K^2 decreases when the hK value of the $SrTiO_3$ buffer layer increases from 0.04 to 0.2 for different IDT configurations except when the IDT is on top of the $KNbO_3$ film with the floating-plane electrode at the interface between the $KNbO_3$ film and the $SrTiO_3$ buffer layer (type 4). However, the change in the coupling coefficient when we increase the buffer thickness is not marked for the type 4 IDT configuration. On the contrary, the change in K^2 is very marked when the IDT is located on top of the $KNbO_3$ film (type 3).

As is known, high quality films are easier to obtain if they are not very thick. According to the formula $hK = h \cdot 2\pi/\lambda$, the real thickness h is about 1.592 μm when the hK value is equal to 1 if the acoustic wavelength λ equals 10 μm. If we select a reasonably large value for the coupling coefficient, for example 1%, as a reference for comparison, we can achieve the optimal selection of IDT configurations. In the preceding results, we know that a larger K^2 can be obtained if the buffer layer is thinner for type 1, type 2 and type 3 IDT configurations. Moreover, the change in the coupling coefficient when we increase the buffer thickness is not marked for the type 4 IDT configuration. Thus, we fixed the hK value of the $SrTiO_3$ buffer layer at 0.04 and the results are arranged in Table I. From Table I we can see the hK value of the $KNbO_3$ film, for which the coupling coefficient is 1%, is smaller than in the other cases when the IDT is located on top of the $KNbO_3$ film (type 3). In the IDT configuration of type 3, the quality of the IDTs and the $KNbO_3$ film are less affected than the other three IDT configurations by the deposition conditions of high growth temperature and high O_2 pressure which are required for preparing the $KNbO_3$ film since IDTs were fabricated after the growth of the $KNbO_3$ film. From the theoretical results and the consideration of the thin-film fabrication process, we can conclude that the layered structure with type 3 IDT configuration is a better choice for device application in the four IDT configurations, and the results could provide useful information for the further development of optical devices, semiconductor devices and SAW devices on the same Si substrate.

4. Conclusion

In this work, we theoretically studied the propagation characteristics of surface acoustic waves in $KNbO_3/SrTiO_3/Si$ structures. The phase velocity and electromechanical coupling coefficient were calculated for different interdigital transducer (IDT) configurations and for various thicknesses of each layer. The results obtained in this study are summarized as follows.

(a) (b) (c) (d)

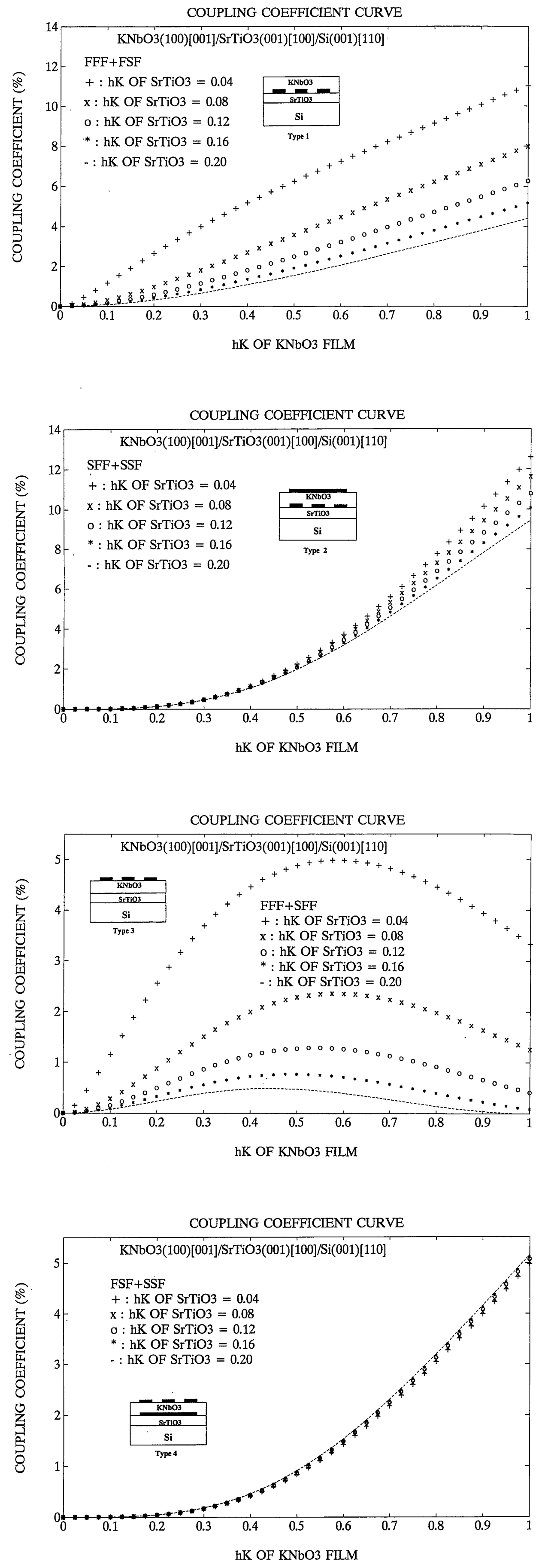

Fig. 4. Calculated coupling coefficient (K^2) curves when the hK values of the $SrTiO_3$ buffer layer are fixed at 0.04, 0.08, 0.12, 0.16 and 0.2 with IDT configurations of (a) type 1, (b) type 2, (c) type 3 and (d) type 4.

Table I. The corresponding hK values and the real thickness of the $KNbO_3$ film for different IDT configurations if the acoustic wavelength λ is equal to 10 μm when the hK value of the $SrTiO_3$ buffer layer is fixed at 0.04.

Electrode structure	hK value of the $kNbO_3$ film for which the coupling coefficient is 1%	Corresponding thickness of the $KNbO_3$ film if the acoustic wavelength λ is equal to 10 μm
TYPE 1	0.090	0.230 μm
TYPE 2	0.375	0.597 μm
TYPE 3	0.090	0.230 μm
TYPE 4	0.525	0.836 μm

(1) The phase velocities (v_p) decrease when the hK value of the $KNbO_3$ film increases from 0 to 1 for a specified thickness of the $SrTiO_3$ buffer layer; they also decrease when the hK value of the $SrTiO_3$ buffer layer increases from 0.04 to 0.2 for a specified thickness of the $KNbO_3$ film.

(2) The value of the coupling coefficient (K^2) can be as high as 10% when the IDT is located at the interface between the $KNbO_3$ film and the $SrTiO_3$ buffer layer, with (type 2) and without (type 1) the floating-plane electrode on top of the $KNbO_3$ film.

(3) Larger K^2 can be obtained if the buffer layer becomes thinner for type 1, type 2 and type 3 IDT configurations. Moreover, the change in the coupling coefficient when we increase the buffer thickness is not marked for the type 4 IDT configuration.

(4) The layered structure with the IDT located on top of the $KNbO_3$ film (type 3) is a better choice for device application among the four IDT configurations since the hK value of the $KNbO_3$ film, for which the coupling coefficient is 1%, is smaller than in the other cases, and the quality of the IDTs and the $KNbO_3$ film is less affected by the deposition conditions than the other three IDT configurations.

1) P. Gunter: Phys. Rep. **93** (1982) 199.
2) M. K. Chun, L. Goldberg and J. F. Weller: Appl. Phys. Lett. **53** (1988) 1170.
3) P. Gunter and F. Micheron: Ferroelectrics **18** (1978) 27.
4) E. Voit, C. Zaldo and P. Gunter: Opt. Lett. **11** (1986) 309.
5) E. Wiesendanger: Ferroelectrics **6** (1974) 263.
6) Y. Uematsu: Jpn. J. Appl. Phys. **13** (1974) 1362.
7) F. P. Strohkendl, P. Gunter, Ch. Buchal and R. Irmscher: J. Appl. Phys. **69** (1991) 84.
8) T. M. Graettinger, S. H. Rou, M. S. Ameen, O. Auciello and A. I. Kingon: Appl. Phys. Lett. **58** (1991) 1964.
9) H. Endo and M. J. Cima: Mater. Res. Soc. Symp. Proc. **310** (1993) 325.
10) B. K. Moon and H. Ishiwara: Jpn. J. Appl. Phys. **33** (1994) 1472.
11) H. Mori and H. Ishiwara: Jpn. J. Appl. Phys. **30** (1991) L1415.
12) H. Ishiwara, N. Tsuji, H. Mori and H. Nohira: Appl. Phys. Lett. **61** (1992) 1459.
13) E. Tokumitsu, K. Itani, B. K. Moon and H. Ishiwara: Jpn. J. Appl. Phys. **34** (1995) 5202.
14) W. Farnell and E. L. Adler: *Physics Acoustics*, eds. W. P. Mason and R. N. Thurston (Academic Press, New York, 1972) Vol. 9, Chap. 2, p. 35.
15) M. Zgonik, R. Schlesser, I. Biaggio, E. Voit, J. Tscherry and P. Gunter: J. Appl. Phys. **74** (1993) 1287.
16) B. A. Auld: *Acoustic Fields and Waves in Solids* (John Wiley & Sons, New York, 1973) Vol. 1, p. 357.
17) B. A. Auld: *Acoustic Fields and Waves in Solids* (John Wiley & Sons, New York, 1973) Vol. 1, p. 57.